CDDpress

www.nature.com/cdd

ARTICLE

Check for updates

BH3 mimetic drugs cooperate with Temozolomide, JQ1 and inducers of ferroptosis in killing glioblastoma multiforme cells

Diane Moujalled[1,2✉], Adam G. Southon[3,6], Eiman Saleh[1,6], Kerstin Brinkmann[1,2], Francine Ke[1,2], Melinda Iliopoulos[1], Ryan S. Cross[1,2], Misty R. Jenkins[1,2], Duong Nhu[1,2], Zilu Wang[1,2], Melissa X. Shi[1], Ruth M. Kluck[1,2], Guillaume Lessene[1,2,4], Stephanie Grabow[1,2,5], Ashley I. Bush[3] and Andreas Strasser[1,2✉]

Glioblastoma multiforme (GBM) is the most common and aggressive form of brain cancer, with treatment options often constrained due to inherent resistance of malignant cells to conventional therapy. We investigated the impact of triggering programmed cell death (PCD) by using BH3 mimetic drugs in human GBM cell lines. We demonstrate that co-targeting the pro-survival proteins BCL-XL and MCL-1 was more potent at killing six GBM cell lines compared to conventional therapy with Temozolomide or the bromodomain inhibitor JQ1 in vitro. Enhanced cell killing was observed in U251 and SNB-19 cells in response to dual treatment with TMZ or JQ1 combined with a BCL-XL inhibitor, compared to single agent treatment. This was reflected in abundant cleavage/activation of caspase-3 and cleavage of PARP1, markers of apoptosis. U251 and SNB-19 cells were more readily killed by a combination of BH3 mimetics targeting BCL-XL and MCL-1 as opposed to dual treatment with the BCL-2 inhibitor Venetoclax and a BCL-XL inhibitor. The combined loss of BAX and BAK, the essential executioners of intrinsic apoptosis, rendered U251 and SNB-19 cells refractory to any of the drug combinations tested, demonstrating that apoptosis is responsible for their killing. In an orthotopic mouse model of GBM, we demonstrate that the BCL-XL inhibitor A1331852 can penetrate the brain, with A1331852 detected in both tumour and healthy brain regions. We also investigated the impact of combining small molecule inducers of ferroptosis, erastin and RSL3, with BH3 mimetic drugs. We found that a BCL-XL or an MCL-1 inhibitor potently cooperates with inducers of ferroptosis in killing U251 cells. Overall, these findings demonstrate the potential of dual targeting of distinct PCD signalling pathways in GBM and may guide the utility of BCL-XL inhibitors and inducers of ferroptosis with standard of care treatment for improved therapies for GBM.

Cell Death & Differentiation (2022) 29:1335–1348; https://doi.org/10.1038/s41418-022-00977-2

INTRODUCTION

Glioblastoma multiforme (GBM) is the most common and aggressive form of brain cancer. It is classified as a grade IV astrocytoma with a median patient survival rate of ~15 months after diagnosis, and an overall 5-year survival of 5% [1]. Current standard of care treatment for GBM patients involves maximal surgical resection followed by chemotherapy with the DNA damage-inducing alkylating agent Temozolomide (TMZ) and radiotherapy. GBM tumours are inherently resistant to conventional therapy, with recurrence almost inevitable within 6–9 months from initial diagnosis. This is in part attributed to a high level of tumour heterogeneity, with glioblastomas exhibiting marked proliferative activity and infiltration of malignant cells into healthy areas of the brain [2]. Subsequent to TMZ, four other agents have been FDA-approved for the treatment of GBM, however, the overall survival for patients has not improved for many years [3]. Therefore, it is critical to identify novel therapeutic targets and develop effective drug combination strategies to treat GBM.

Apoptosis, a form of programmed cell death (PCD), is vital for normal embryonic development and maintenance of tissue homoeostasis. Apoptosis is used for the removal of damaged, infected or obsolete cells [4, 5]. This cell death pathway is regulated by the balance between anti-apoptotic and pro-apoptotic B cell lymphoma-2 (BCL-2) family proteins and can be induced via the mitochondrial (aka intrinsic) or the death receptor (aka extrinsic) signalling pathways [5]. Pro-apoptotic BH3-only proteins (BIM, PUMA, BID, BMF, BAD, HRK, BIK, NOXA) are transcriptionally or post-transcriptionally upregulated in response to intracellular stressors, such as DNA damage, ER stress or growth factor deprivation. They initiate apoptosis by binding to and inhibiting the anti-apoptotic BCL-2 family members, including BCL-2, BCL-XL, MCL-1, BCL-W and A1/BFL-1 [6, 7]. The binding of BH3-only proteins to the anti-apoptotic BCL-2 proteins frees BAX and BAK, the effectors of apoptosis, from their restraint by the anti-apoptotic BCL-2 proteins, thereby unleashing the caspase cascade that dismantles the dying cells [4, 5, 8]. In GBM, malignant

[1]The Walter and Eliza Hall Institute, Melbourne, VIC, Australia. [2]Department of Medical Biology, The University of Melbourne, Parkville, VIC 3010, Australia. [3]Melbourne Dementia Research Centre, Florey Institute of Neuroscience and Mental Health, The University of Melbourne, Melbourne, VIC, Australia. [4]Department of Pharmacology and Therapeutics, The University of Melbourne, Parkville, VIC 3010, Australia. [5]Present address: Vividion Therapeutics, San Diego, CA 92121, USA. [6]These authors contributed equally: Adam G. Southon, Eiman Saleh. ✉email: dmoujalled@wehi.edu.au; strasser@wehi.edu.au

Edited by G Melino

Received: 23 July 2021 Revised: 3 March 2022 Accepted: 4 March 2022
Published online: 24 March 2022

cells display inherent defects in apoptotic cell death, and are therefore resistant to diverse cytotoxic agents [9]. It is thought that this contributes to the failure of conventional standard-of-care treatment in GBM. Human glioblastoma cells were shown to express higher levels of the pro-survival proteins BCL-2 and BCL-XL compared to non-neoplastic glial cells [10]. Of note, it was reported that RNA interference-mediated reduction in BCL-2 or BCL-XL was able to cause caspase dependant killing of glioblastoma cells in culture [10]. High levels of BCL-XL have been associated with rapid disease progression and poor survival of glioblastoma patients. Therefore, BCL-XL has been proposed as a marker of therapy resistance in this malignancy [11].

BH3 mimetic drugs are small molecule agents that bind to and antagonise anti-apoptotic BCL-2 family proteins, directly triggering the apoptosis machinery in a BAX/BAK dependant manner [7, 12]. The BH3-mimetics S63845 [13], A1331852 [14] and Venetoclax/ABT-199 [15] selectively target MCL-1, BCL-XL and BCL-2, respectively [7]. The BCL-2 inhibitor Venetoclax/ABT-199 is approved by the FDA and many other regulatory authorities for the treatment of Chronic Lymphocytic Leukaemia (CLL) and Acute Myeloid Leukemia (AML) [16]. In pre-clinical studies, the MCL-1 inhibitor S63845 was shown to effectively kill a range of B cell lymphoma, multiple myeloma and AML derived cell lines in culture and even in vivo [13]. However, this [13] and other MCL-1 inhibitors [17–19] mostly had only modest impact as single agents on cell lines derived from solid cancers, although they substantially enhanced the therapeutic effect of inhibitors of oncogenic kinases and diverse standard chemotherapeutic drugs. The BCL-XL inhibitor A1331852 was shown to kill diverse lymphoma and leukaemia-derived cell lines and delayed the progression of acute lymphocytic leukaemia (ALL) in xenograft mouse models [20]. Combined targeting of BCL-XL and MCL-1 was reported to synergise in killing melanoma cells in 2D and 3D cell culture models [21] and in cervical cancer derived cell lines [22]. However, the safety of this combination therapy is a concern given that loss of only single alleles of *Bcl-x* and *Mcl-1* causes fatal early neonatal craniofacial defects [23], and that combined loss of BCL-XL and MCL-1 specifically in hepatocytes causes liver failure [24]. Nonetheless, it is anticipated that careful refinement of the therapeutic window of existing BH3 mimetic drugs and the generation of BH3 mimetics conjugated to an antibody that selectively targets malignant cells will lead to improvements in the treatment of brain cancer and other solid cancers [25].

Ferroptosis refers to a form of iron-dependent necrotic PCD, characterised by overwhelming lipid peroxidation [26]. In cells undergoing ferroptosis, mitochondria appear smaller than normal with increased membrane density [26], while classical features of apoptosis, such as mitochondrial cytochrome *c* release, caspase activation, and chromatin fragmentation are not observed [26]. Ferroptosis can be induced by small molecules, such as erastin, which inhibits the cystine transport receptor systemXc^- (xCT), thereby diminishing intracellular glutathione levels. RAS-selective lethal small molecule 3 (RSL3), functions as a covalent inhibitor of glutathione peroxidase 4, a glutathione dependent enzyme that functions to inhibit the formation of lipid peroxides and thereby induces ferroptosis [26]. Overexpression of xCT in glioblastoma was shown to be associated with a cancer-stem cell like phenotype which may contribute to increased resistance to chemotherapeutic drugs [27]. Inhibition of xCT by erastin or the clinically approved sulfasalazine, was reported to potentiate the impact of TMZ in human GBM cells [28]. Moreover, in a diffuse large B cell lymphoma xenograft mouse model, imidazole ketone erastin, a second-generation inducer of ferroptosis, resulted in glutathione depletion, lipid peroxidation, and the induction of markers of ferroptosis, and this treatment slowed tumour growth both in vitro and in vivo [29].

In the present study, we assessed the impact of combining standard of care treatment for GBM with BH3 mimetic drugs in human GBM cell lines. We demonstrate that co-targeting the two pro-survival proteins BCL-XL (with A1331852) and MCL-1 (with S63845) was more potent at triggering cell death in SNB-19, SNB-75, U251, SF268, SF295 and SF539 GBM cell lines compared to conventional therapy. We demonstrate that the BCL-XL inhibitor, A1331852 can penetrate and accumulate in the brain in an orthotopic mouse model of GBM. We also show that the combination of BH3 mimetics selectively targeting MCL-1 and BCL-XL, or BCL-XL inhibitors combined with TMZ, or the bromodomain inhibitor JQ1 robustly enhanced the killing of GBM cells in vitro. Induction of apoptosis was demonstrated by cleavage of caspase-3 and its substrate Poly ADP-ribose polymerase 1 (PARP1). Accordingly, U251 and SNB-19 cells lacking both BAX and BAK, the essential effectors of apoptosis, were refractory to the aforementioned treatment combinations. We also demonstrate that combined treatment of GBM cells with BH3 mimetics targeting MCL-1 and BCL-XL and small molecule inducers of ferroptosis, such as erastin or RSL3, enhanced the killing of U251 cells compared to activating only one PCD pathway. Thus, combination regimens of dual triggering of apoptosis and ferroptosis may be considered as a strategy for improved therapies for GBM.

RESULTS

Co-targeting of MCL-1 and BCL-XL with BH3 mimetic drugs kills glioblastoma cells more potently than treatment with TMZ or the bromodomain inhibitor JQ1

We first assessed the expression of the pro-survival BCL-2 family members, MCL-1, BCL-XL and BCL-2, in a panel of 6 human glioblastoma cell lines: SNB-19, SNB-75, U251, SF-268, SF-295 and SF-539. MCL-1 was abundantly expressed in most GBM cell lines with the levels comparable to those seen in the HEK293 human embryonic kidney cell line and A357 human melanoma cells (Supplementary Fig. S1a). BCL-XL and BCL-2 were detected at lower levels (Supplementary Fig. S1a).

Previous studies have demonstrated that targeting pro-survival proteins with BH3 mimetic drugs, such as the MCL-1 inhibitor S63845 [13], the BCL-XL inhibitor A1331852 [14] or the BCL-2 inhibitor Venetoclax/ABT-199 [15] can effectively kill a broad range of cancer derived cell lines as single agent or in combination [7, 13, 22]. The utility of BH3 mimetic drug treatment has not yet been explored in human GBM cells. Therefore, we tested the impact of combining the MCL-1 and BCL-XL inhibitors S63845 and A1331852 on the viability and growth of GBM cells in culture. Combined treatment with S63845 and A1331852 for 5 days exerted robust anti-proliferative effects in GBM cells (IC_{50} in the low nM range for all six cell lines assessed), with U251 cells highly sensitive to the combination treatment (IC_{50} < 100 nM), (Supplementary Fig. S1b), as measured by the Cell-Titre Glo viability assay. These effects were more pronounced than the modest single agent effects induced by TMZ or JQ1 (Fig. 1a–c and Supplementary Fig. S1b). We also tested the ability of BH3 mimetic drugs, used as single or dual agent treatment for 5 days, to induce apoptosis in U251 and SNB-19 GBM cells by staining with Annexin V and DAPI followed by flow cytometric analysis. Only single agent treatment with the BCL-XL inhibitor A1331852 induced significant apoptosis in U251 and SNB-19 cells, whereas only little apoptotic death was observed after treatment with the MCL-1 inhibitor S63845 or the BCL-2 inhibitor Venetoclax/ABT-199 (Fig. 2a, b). Dual treatment with S63845 and A1331852 induced robust apoptosis (Fig. 2a, b), with U251 cells being more sensitive to 48 h of this treatment (IC_{50} 0.6 μM) compared to SNB-19 cells (IC_{50} 2.2 μM) (Supplementary Fig. S2a, c). Analysis of cell viability at earlier timepoints revealed that combinations of S63845 plus A1331852 as low as 0.1 μM each caused significant killing of U251 cells within 16 h and SNB-19 cells within 24 h of treatment in vitro (Fig. 2c, d). Cell death in response to these combination treatments was also evaluated by using the InCucyte live cell

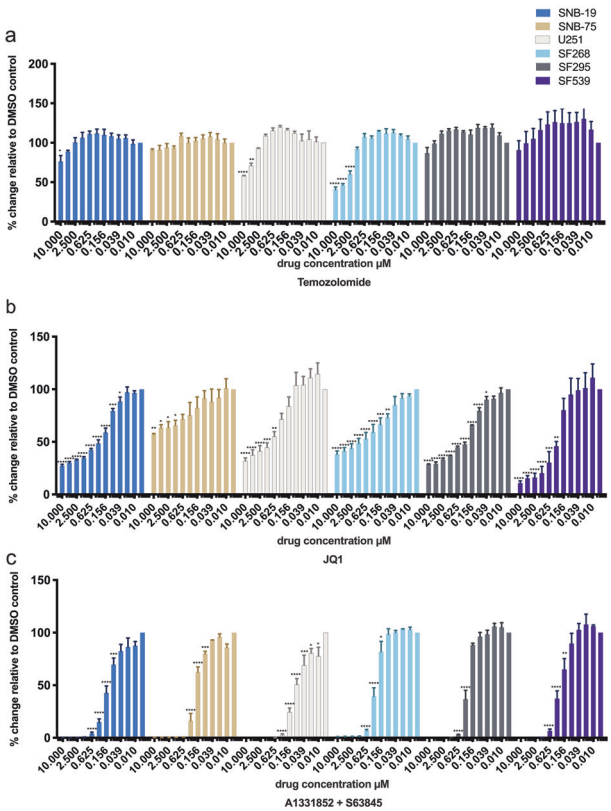

Fig. 1 BH3 mimetic drugs targeting MCL-1 and BCL-XL kill GBM cells more potently compared to TMZ or JQ1 monotherapy. Viability of the human GBM cell lines, SNB-19, SNB-75, U251, SF-268, SF-295 and SF-539, after treatment with the indicated concentrations of **a** TMZ, **b** JQ1 or **c** dual treatment with S63845 (MCL-1 inhibitor) plus A1331852 (BCL-XL inhibitor). ATP levels were determined after 5 days of continuous treatment using the CellTiter-Glo® assay with data presented relative to DMSO (vehicle control) treated cells. $n = 3$ independent experiments, data are presented as mean ± S.D. One-way ANOVA with the Dunnett's multiple comparisons tests relative to DMSO vehicle treated cells. *$P < 0.05$, **$P <$,0.01, ***$P < 0.001$, ****$P < 0.0001$.

imaging platform, where we found that the combination of A1331852 and S63845 rapidly caused an increase in propidium iodide signal and loss of cell confluency in a dose dependant manner (Supplementary Fig. S3a, b, e, f). In contrast, treatment with S63845 plus Venetoclax induced cell death more slowly and confluency of U251 cells was only reduced at higher doses (Supplementary Fig. S3c, d, g, h). Collectively, these results demonstrate that co-targeting MCL-1 and BCL-XL is more effective at killing GBM cells compared to standard of care therapy.

Combination treatment of TMZ or JQ1 with the BCL-XL inhibitor A1331852 potently kills glioblastoma cells

Current standard of care treatment for GBM patients includes chemotherapy with the DNA damage-inducing alkylating agent TMZ [30]. Inhibition of BET (bromodomain and extra-terminal) bromodomain proteins with the small molecule inhibitor JQ1 has been reported to regulate the DNA damage response in several cancer cell lines in vitro, and to promote G1 cell cycle arrest and dissipation of the mitochondrial membrane potential [31–33]. Of note, inhibition of BET bromodomain proteins was reported to have anti-tumour effects in mouse models of glioma [34]. Co-treatment of U87MG and GL261 glioma cells with TMZ and the BET inhibitor JQ1 caused substantial DNA damage and tumour cell killing in vitro and slowed tumour expansion in mice [35]. It was previously shown that combined treatment with JQ1 and the BH3 mimetic ABT-263, a potent inhibitor of BCL-2, BCL-XL and BCL-W, caused substantial apoptosis in glioma cells in vitro, and this was accompanied by an increase in the pro-apoptotic BH3-only protein NOXA and activation of caspases [33, 36].

To explore the impact of combinations of BH3 mimetic drugs with TMZ or JQ1 on the killing of GBM cells, we assessed the viability of U251 cells after 5 days of single agent and combination treatments by staining with Annexin V and DAPI, followed by flow cytometric analysis. Significant death was observed in cells treated with 50 μM TMZ or 1 μM JQ1 as single agents. Notably, the BCL-XL inhibitor A1331852 (but none of the other BH3 mimetic drugs tested) co-operated with TMZ as well as JQ1 in the killing of U251 cells (Fig. 3a).

To ascertain the effect of single agent and combination treatments with A1331852, TMZ and JQ1 on cell cycle progression, cell cycle distribution was assessed in U251 and SNB-19 cells by DAPI staining and flow cytometric analysis to measure DNA content (Fig. 3b, c and Supplementary Table 1). Treatment of U251 cells with 50 μM TMZ alone and when combined with 1 μM of the BCL-XL inhibitor A1331852 caused a significant reduction of cells in the G1 phase (vehicle control treated: 62.6%, compared to TMZ treated: 27.7% and TMZ plus A1331852 treated: 24.2%). Treatment with TMZ and A1331852 also caused a substantial increase of U251 cells in the sub-G1 phase (dying cells; vehicle control treated: 10.1% compared to TMZ plus A1331852 treated: 26.3%), consistent with an increase in apoptotic cells. Treatment with TMZ alone induced G2/M cell cycle arrest in U251 cells (vehicle control treated: 12.8% compared to TMZ treated: 50.5%) and SNB-19 cells (vehicle control treated: 13.4% compared to TMZ treated: 25.8%). In SNB-19 cells, the combination of TMZ plus A1331852 also promoted significant G2/M cell cycle arrest (vehicle control treated: 13.4% compared to TMZ plus A1331852 treated: 23.2%) (Fig. 3b, c and Supplementary Table 1). We did not observe significant effects of JQ1 on cell cycle progression in U251 and SNB-19 cells at 48 h post-treatment as single agent or when combined with A1331852. These results reveal that TMZ promotes G2/M cell cycle arrest in U251, and SNB-19 cells and enhances apoptosis when combined with a BCL-XL inhibitor.

Activation of caspase-3 and cleavage of PARP1 in response to dual treatment with MCL-1 inhibitor combined with BCL-XL inhibitor, JQ1 combined with BCL-XL inhibitor or TMZ combined with either BH3 mimetic drug

The mechanism underlying the anti-tumour effects of TMZ is thought to be due to its DNA alkylating properties, delivering a methyl group to purine bases of DNA (O6-guanine; N7-guanine and N3-adenine), thereby eliciting DNA damage to cause apoptosis [37]. It has also been reported that TMZ induces autophagy in U251 cells, thereby attenuating cell migration and reducing cell viability [38]. JQ1 has been reported to impact the DNA damage response, triggering G1 cell cycle arrest [31, 32]. The promising clinical utility of BH3 mimetics is encompassed by their ability to directly activate the apoptosis machinery in cancer cells by inhibiting anti-apoptotic BCL-2 family members, therefore bypassing the requirement for upstream initiators of apoptosis, such as the tumour suppressor p53 [39]. We assessed the ability of single and dual agent BH3 mimetic drug treatments or TMZ and JQ1 as single agents and in combination with BH3 mimetics to trigger apoptosis in U251 and SNB-19 cells. This was done by examining the amounts of cleaved (i.e. activated) caspase-3 and the proteolysis of its substrate PARP1, both markers of apoptosis. Abundant cleavage of caspase-3 (p19 and p17 fragments detected by Western blotting) and accumulation of a cleaved PARP1 fragment were detected in U251 and SNB-19 cells after combined treatment with 1 μM of each, the BCL-XL inhibitor A1331852 and the MCL-1 inhibitor S63845 overnight (Fig. 4a, c and Supplementary Fig. S4a, d). U251 and SNB-19 cells were also subjected to single and dual agent treatment with 50 μM

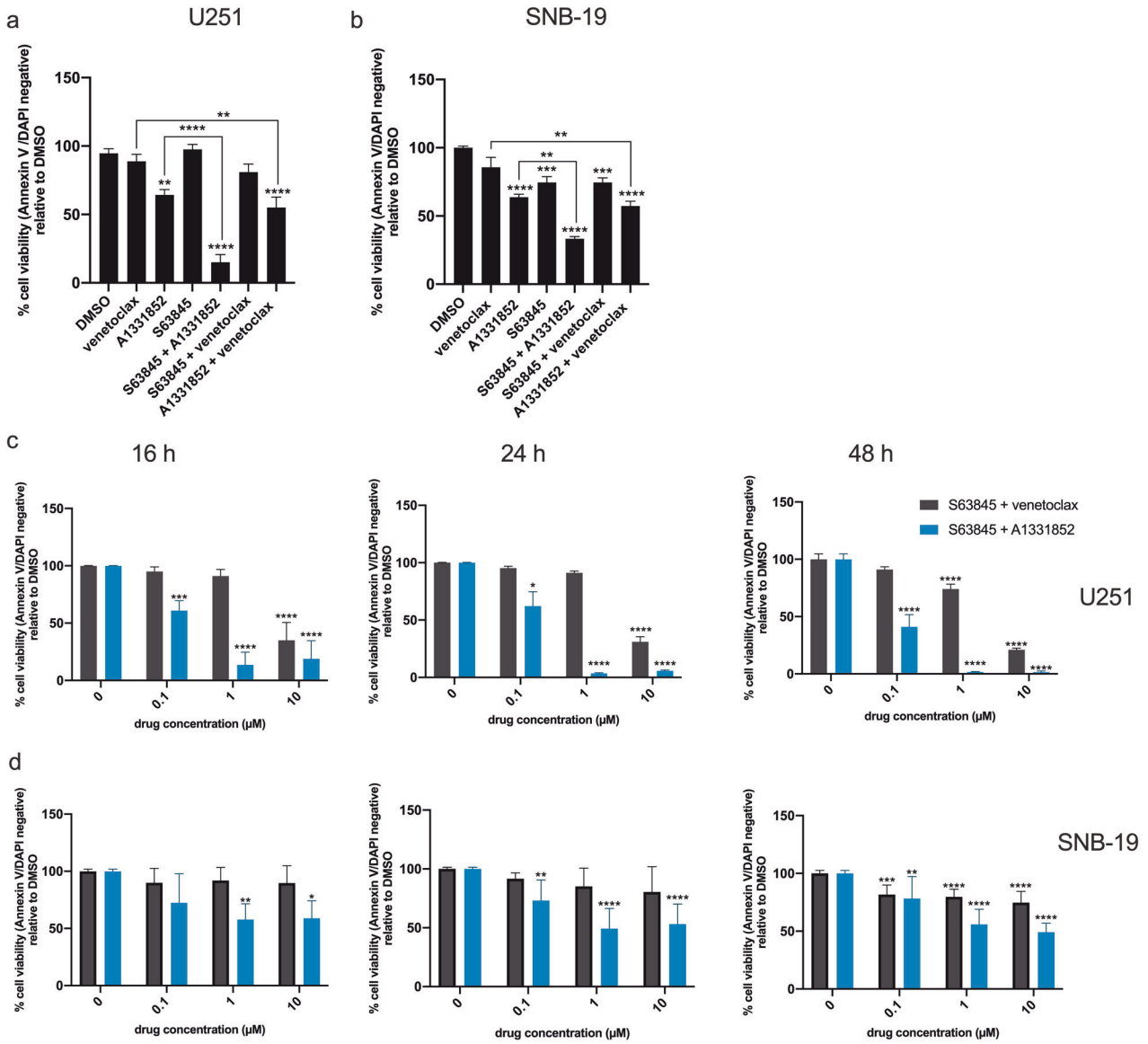

Fig. 2 Combination treatments with BH3 mimetic drugs targeting MCL-1, BCL-XL or BCL-2 causes increased apoptosis of GBM cells compared to single agent treatment. a, b U251 and SNB-19 cells were treated as indicated with BH3 mimetic drugs as single agents or combinations of BH3 mimetic drugs at 1 μM each for 5 days. Cell viability was determined by staining with Annexin V plus DAPI followed by flow cytometric analysis. n = 3 independent experiments, data are presented as mean ± s.d. One-way ANOVA with the Dunnett multiple comparison test relative to DMSO (vehicle control) treated cells. **c, d** U251 or SNB-19 cells were treated with the indicated drug combinations for 16, 24 or 48 h. Cell viability was determined by staining with Annexin V plus DAPI followed by flow cytometric analysis. $n = 3$ independent experiments, data are presented as mean ± s.d. One-way ANOVA with the Tukey's multiple comparisons tests relative to DMSO (vehicle control) treated cells or as indicated between treatment groups. *$P < 0.05$, ***$P < 0.001$, ****$P < 0.0001$.

TMZ, 1 μM JQ1 and 1 μM BH3 mimetics for 5 days. In U251 cells, abundant cleavage (activation) of caspase-3 and accumulation of cleaved PARP1 were observed in response to TMZ as single agent, and in combination with S63845, A1331852 or Venetoclax (Fig. 4b and Supplementary Fig. S4b, c). JQ1 treatment alone did not induce cleavage of caspase-3 or PARP1, however, cleaved (activated) caspase-3 and cleaved PARP1 were abundant when JQ1 was combined with the BCL-XL inhibitor A1331852 (Fig. 4b). In SNB-19 cells, we observed accumulation of cleaved caspase-3 in response to TMZ as single agent, and in combination with S63845, A1331852 or Venetoclax, and in response to dual treatment with JQ1 and A1331852 (Fig. 4d and Supplementary Fig. S4e). In the presence of the broad-spectrum caspase inhibitor QVD-OPH, no cleavage (activation) of caspase-3 or its substrate PARP1 was detected in U251 cells treated with single or dual agent BH3 mimetic treatment or TMZ and JQ1 combined with BH3 mimetic drugs (Supplementary Fig. S5a, b). Moreover, QVD-OPH protected U251 and SNB-19 cells from apoptosis (shown by staining with Annexin V and DAPI) induced by BH3 mimetic drugs and JQ1 as single agents or combinations of these agents (Supplementary Fig. S6a, b, c, d). However, despite the addition of QVD-OPH, U251 cells showed staining with Annexin V and DAPI after treatment with TMZ as single agent or in combination with BH3 mimetic drugs (Supplementary Fig. S6b), demonstrating that this death can occur in the absence of caspase activity. Overall, these results demonstrate that JQ1 can effectively trigger apoptosis when combined with the BCL-XL inhibitor A1331852 whereas TMZ alone or when combined with BH3 mimetic drugs, in particular an inhibitor of BCL-XL, can trigger cell death with hallmarks of apoptosis but also through a caspase independent process.

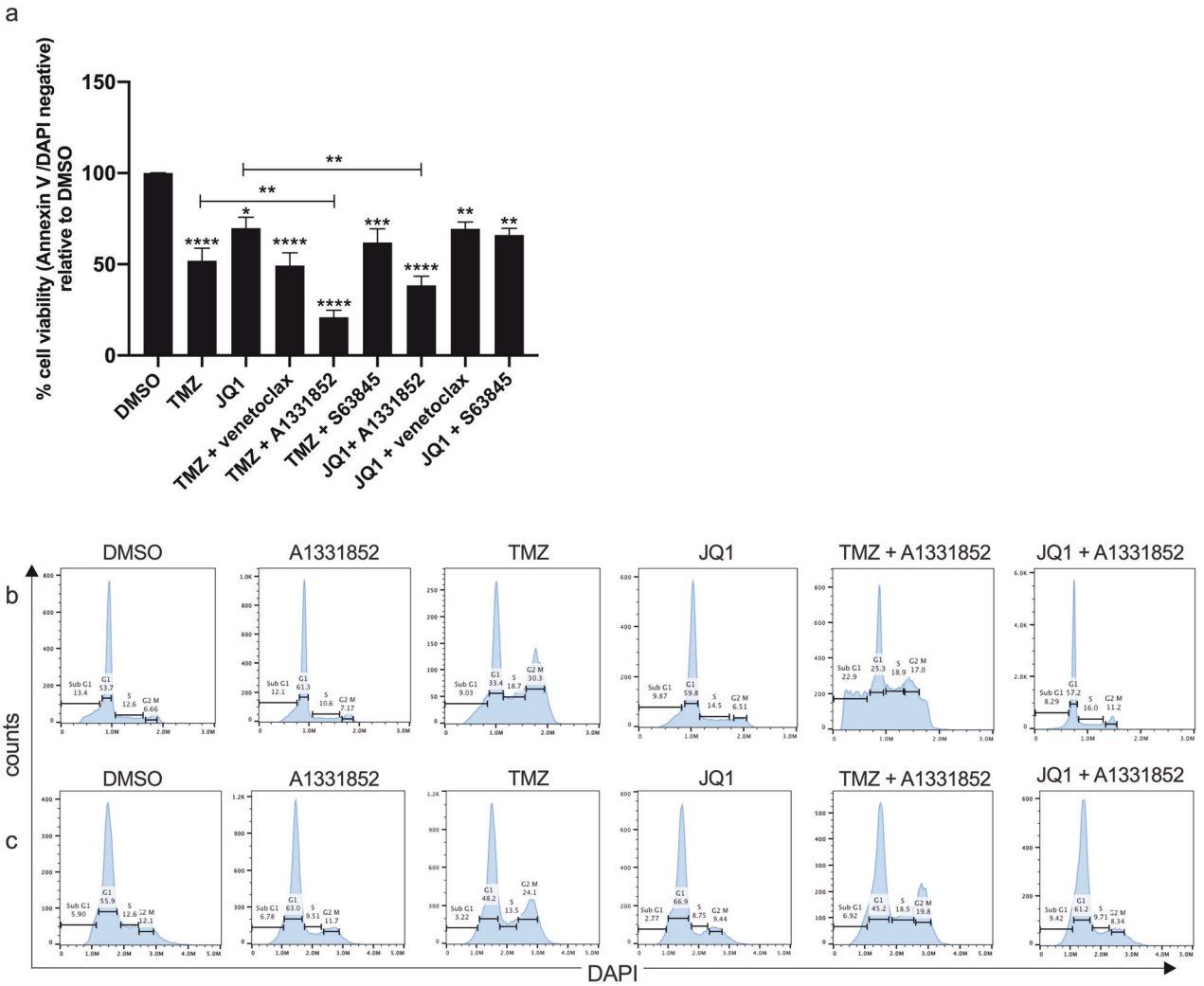

Fig. 3 Combinations of BH3 mimetic drugs with TMZ or JQ1 cause increased killing of GBM cells compared to TMZ or JQ1 monotherapy. **a** U251 cells were treated for 5 days with 1 μM A1331852 (BCL-XL inhibitor), 1 μM S63845 (MCL-1inhibitor), 1 μM Venetoclax (BCL-2 inhibitor); 50 μM TMZ; 1 μM JQ1 as single agents or with the indicated drug combinations. Cell viability was determined by staining with Annexin V plus DAPI followed by flow cytometric analysis. $n = 3$ independent experiments, data are presented as mean ± s.d. One-way ANOVA with the Tukey's multiple comparisons tests relative to DMSO (vehicle control) treated cells or as indicated. *$P < 0.05$, **$P < ,0.01$, ***$P < 0.001$, ****$P < 0.0001$. **b** Effect of A1331852, TMZ and JQ1 as single agents or combination treatments as indicated on cell cycle progression. U251 and SNB-19 cells were treated for 48 h with 1 μM A1331852, 1 μM JQ1 or 50 μM TMZ. DMSO was used as vehicle control. Cells were fixed in 70% ethanol followed by DAPI staining and flow cytometric analysis. Percentages of cells in the sub-G1 (dying), G1, S and G2/M phases are indicated. Histograms shown are representative of results from three independent experiments.

The combined absence of BAX and BAK renders U251 and SNB-19 glioblastoma cells resistant to combined treatment with TMZ plus BH3 mimetic drugs

The multi-BH domain pro-apoptotic proteins BAX and BAK are the essential effectors of the intrinsic pathway of apoptosis [5, 40]. Accordingly, cells lacking BAX and BAK are refractory to diverse agents that kill cells by inducing apoptosis [13, 41]. For example, the combined deletion of BAX and BAK using CRISPR/Cas9 technology rendered tumour-derived cell lines resistant to the MCL-1 inhibitor S63845 [13]. To determine whether loss of BAX and BAK can protect GBM cells from apoptosis triggered by BH3 mimetic drugs, TMZ, JQ1 and combinations thereof, we employed CRISPR/Cas9 technology to generate U251 and SNB-19 cells deficient in BAX and BAK. Treatment with doxycycline to induce expression of the guide RNAs (gRNA) targeting *Bax* and *Bak*, resulted in a significant reduction of BAX and BAK in U251 and SNB-19 cells, as confirmed by Western blotting (Fig. 5a). BAX/BAK double knock-out (DKO) U251 and SNB-19 cells were significantly protected from cell death induced by the combination of the MCL-1 inhibitor S63845 plus the BCL-XL inhibitor A1331852 (Fig. 5b and Supplementary Fig. S7c). Significant rescue in cell viability was also observed in BAX/BAK DKO U251 cells treated with combinations of TMZ plus A1331852, or combinations of JQ1 with A1331852, Venetoclax/ABT-199 or S63845 (Fig. 5c). Similarly, BAX/BAK DKO SNB-19 cells, were significantly protected from killing induced by treatment with combinations of TMZ with A1331852, Venetoclax/ABT-199 or S63845 and JQ1 combined with A1331852 (Fig. 5d). It appears that TMZ as a single agent caused comparable loss of cell viability in control and BAX/BAK DKO U251 and SNB-19 cells. This indicates that TMZ must be able to also trigger cell death processes in addition to intrinsic apoptosis. Notably, parental U251 cells were more sensitive to cell death induced by JQ1 compared to the SNB-19 cells (Fig. 5c, d). We also generated single cell clones of SNB-19 cells by cell sorting and treated them with doxycycline to induce expression of guide RNAs (gRNA) targeting *Bax* and *Bak*. These clones were expanded and assessed for the deletion of BAX and BAK by Western blotting (Supplementary Fig. S8a). Efficient deletion of BAX and BAK was

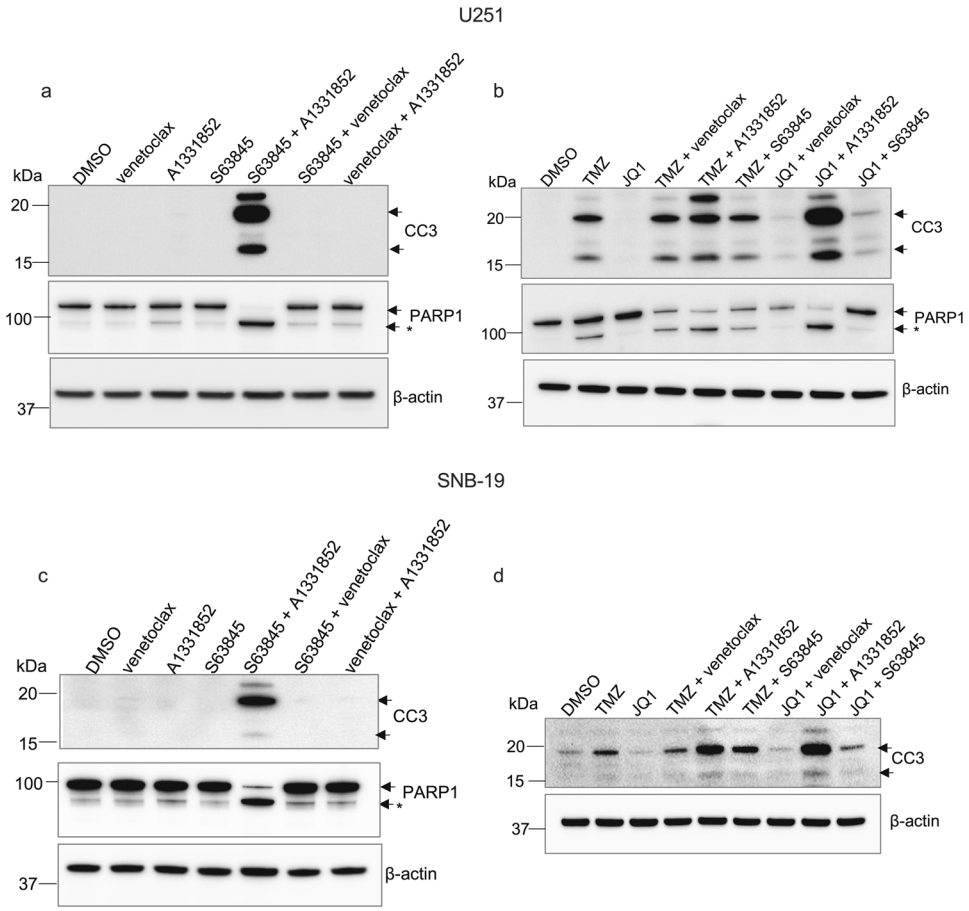

Fig. 4 Cleavage of caspase-3 and PARP1, markers of apoptosis, is seen in U251 and SNB-19 cells after treatment with TMZ or JQ1 plus BH3 mimetic drugs. a, **c** Western blot analysis of lysates from U251 or SNB-19 cells that had been treated with 1 μM A1331852 (BCL-XL inhibitor), 1 μM Venetoclax/ABT-199 (BCL-2 inhibitor) or 1 μM S63845 (MCL-1 inhibitor) for 16 h as single agents or the indicated drug combinations. **b**, **d** Western blot analysis of lysates from U251 or SNB-19 cells that had been treated for 4 days with 1 μM A1331852, 1 μM S63845, 1 μM Venetoclax/ABT-199, 50 μM TMZ or 1 μM JQ1. Membranes were probed for cleaved (activated) caspase-3 (CC3; p19, 17 fragments indicated) and cleaved PARP1. * indicates cleaved PARP1 fragment. Probing for β-actin was used as a loading control.

observed in clones #4, 5, 7 and 9. As expected, clone #4 was profoundly resistant to treatment with combinations of TMZ or JQ1 with BH3 mimetic drugs (Supplementary Fig. 8b). BAX/BAK DKO U251 cells were also significantly protected from JQ1 induced cell death (Fig. 5c). The rescue in cell viability in BAX/BAK DKO U251 and SNB-19 cells was supported by observations that in these cells we detected no (or only little) cleavage of caspase-3 and PARP1 after dual treatment with S63845 plus A1331852, TMZ combined with BH3 mimetic drugs or JQ1 combined with A1331852 (Fig. 5e, f and Supplementary Fig. S7a, b). BAX or BAK single knock out (SKO) U251 cells were also generated by CRISPR/Cas9, with efficient deletion of BAX or BAK verified by Western blot analysis (Supplementary Fig. S9a). BAX SKO but not BAK SKO U251 cells were resistant to treatment with S63845 plus A1331852, demonstrating that in these cells, BAX is more critical than BAK for MCL-1 inhibitor plus BCL-XL inhibitor induced apoptosis (Supplementary Fig. S9b, c). BAK SKO U251 cells but not BAX SKO U251 cells were protected from killing induced by TMZ alone and TMZ combined with A1331852 (Supplementary Fig. S9d, e), demonstrating BAK is more critical than BAX in the killing of these cells by TMZ.

The BCL-XL inhibitor A1331852 can penetrate the brain and enter brain tumour tissue in an orthotopic mouse model of GBM

The ability of small molecule agents to penetrate the brain remains a major challenge for the treatment of GBM. While TMZ can penetrate the brain due to its small size and lipophilic properties, many anti-cancer agents do not exhibit these characteristics. To investigate whether the BCL-XL inhibitor A1331852 can penetrate and accumulate in the brain of healthy and tumour bearing mice, we first assessed the concentration of A1331852 in the brain and plasma of healthy (i.e. not bearing tumours) NOD/SCID/$\gamma c^{-/-}$ mice, 1 h and 4 h post-drug administration at 25 mg/kg body weight by Ultra Performance Liquid Chromatography (UPLC). Based on the brain to plasma ratio, we conclude that A1331852 was not present at a significant concentration in the brain of healthy mice, and therefore did not adequately penetrate the brain to detectable levels (Supplementary Table 2). We next ascertained whether A1331852 can penetrate the brain of tumour bearing mice. For this, NOD/SCID/$\gamma c^{-/-}$ mice were intracranially injected with U251 human GBM cells harbouring an mCherry-luciferase reporter to establish an orthotopic mouse model of GBM as previously described [42]. Engraftment of tumour cells was detected on day 7 by bioluminescent imaging (Fig. 6a). Following daily treatment for 5 days with 50 mg/kg body weight A1331852, there was a marked decrease in platelet numbers (Fig. 6b), consistent with on-target thrombocytopenia caused by inhibition of BCL-XL [43], thereby confirming successful administration of the drug. The brain was less exposed to A1331852 compared to the liver and spleen, however, this drug was detected in malignant as well as healthy tissue in the brain at concentrations above the binding affinity for

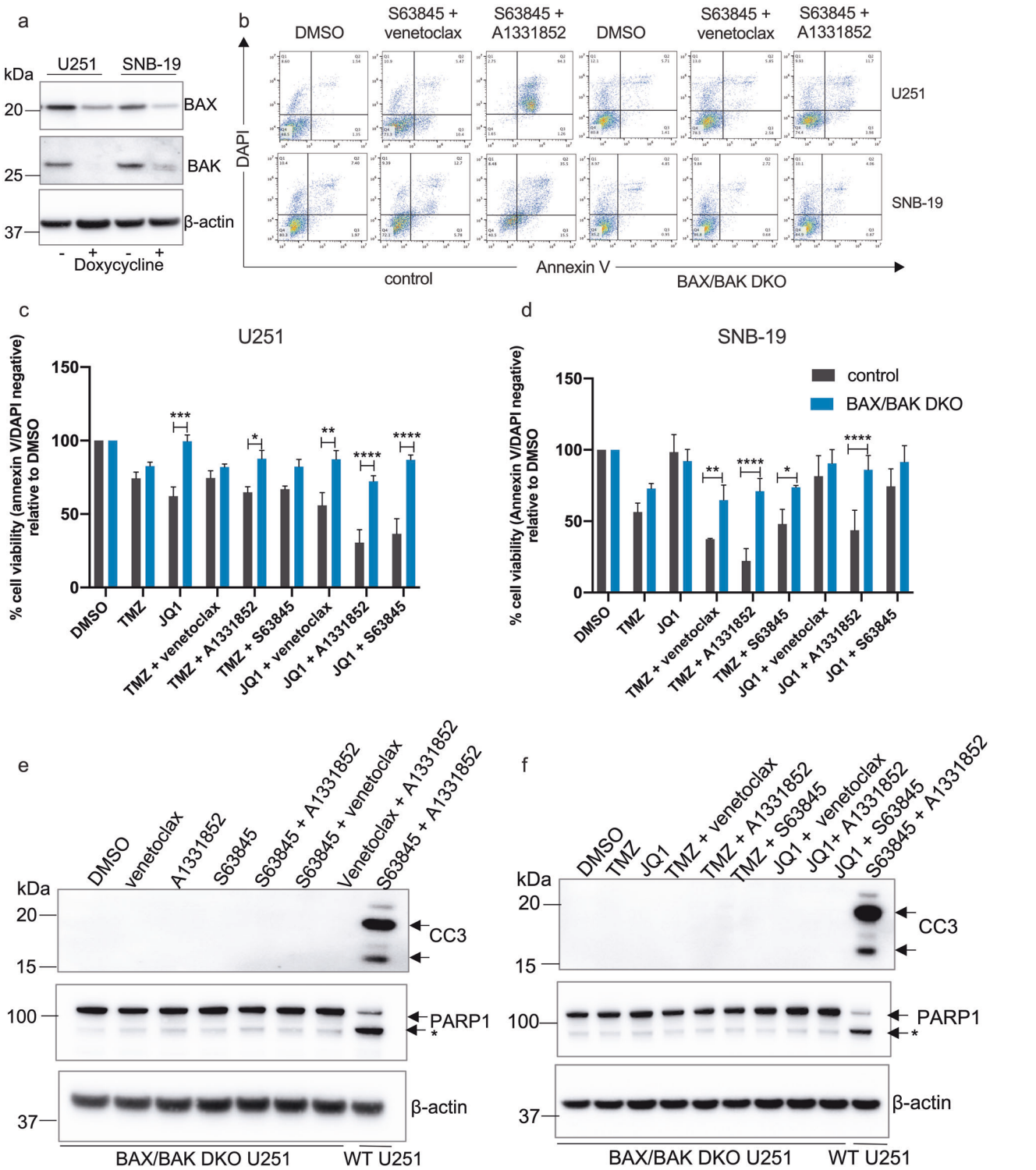

BCL-XL (Fig. 6c, Supplementary Table 3), which is in the low nanomolar range [14]. This warrants future studies to assess the in vivo therapeutic impact of A1331852 in preclinical models of GBM.

Inducers of ferroptosis cooperate with BH3 mimetic drugs in the killing of GBM cells

Ferroptosis represents a form of iron-dependant PCD characterised by overwhelming lipid peroxidation [26]. Small molecules, such as erastin and RSL3, can induce ferroptosis. Erastin inhibits xCT, thereby diminishing intracellular glutathione levels and promoting cell death, whereas RSL3 covalently binds to and inhibits GPX4 and thereby induces ferroptotic cell death, without affecting glutathione levels in the presence of liproxstatin-1 (Supplementary Fig. S10a-d). In vitro, the effects of lipid peroxidation can be neutralised by iron chelators, such as deferoxamine (DFO), and lipophilic radical traps, such as ferrostatin-1 or liproxstatin-1, and these agents can thereby inhibit ferroptosis [44]. In U251 cells, both erastin and RSL3 caused an accumulation of toxic lipid reactive oxygen species (ROS) with ensuing lipid peroxidation (Supplementary Fig. S11) [26], with a

Fig. 5 U251 and SNB-19 cells lacking both BAX and BAK, the essential effectors of apoptosis, are profoundly resistant to killing by combination treatments with TMZ or JQ1 with BH3 mimetic drugs. a Western blot analysis of lysates from U251 or SNB-19 cells that had been left untreated or treated with 1 μg/mL doxycycline for 5 days to induce expression of *Bax* and *Bak* sgRNAs. Blots were probed for BAX, BAK and β-actin, the latter used as a loading control. **b**, **c**, **d** U251 or SNB-19 cells were left untreated (control) or treated with 1 μg/mL doxycycline for 5 days to induce sgRNAs for *Bax* and *Bak*. **b** Cells were then treated for 48 h with 1 μM A1331852 (BCL-XL inhibitor), 1 μM S63845 (MCL-1 inhibitor) or 1 μM Venetoclax/ABT-199 (BCL-2 inhibitor) with the indicated combinations. Shown are representative dot plots following staining with Annexin V plus DAPI followed by flow cytometric analysis. **c**, **d** Cells were treated for 5 days with 1 μM A1331852 (BCL-XL inhibitor), 1 μM S63845 (MCL-1 inhibitor), 1 μM Venetoclax/ABT-199 (BCL-2 inhibitor), 50 μM TMZ, 1 μM JQ1 as single agents or with the indicated drug combinations. Cell viability was determined by staining with Annexin V plus DAPI followed by flow cytometric analysis. $n = 3$ independent experiments; data are presented as mean ± s.d. Two-way ANOVA with the Bonferroni's multiple comparisons tests. $^{*}P < 0.05$, $^{**}P < 0.01$, $^{***}P < 0.001$, $^{****}P < 0.0001$. **e** Western blot analysis of lysates from BAX/BAK DKO U251 cells that had been treated for 16 h with 1 μM A1331852, 1 μM Venetoclax/ABT-199 or 1 μM S63845 as single agents or with the combinations of agents indicated. **f** Western blot analysis of lysates from BAX/BAK DKO U251 cells that had been treated for 5 days with 1 μM A1331852, 1 μM S63845, 1 μM Venetoclax/ABT-199, 50 μM TMZ or 1 μM JQ1. Membranes were probed for cleaved (activated) caspase-3 (CC3; p19, 17 fragments indicated) and cleaved PARP1. * indicates cleaved PARP1 fragment. Probing for β-actin was used as a loading control. Lysates from parental U251 cells that had been treated with 1 μM A1331852 plus 1 μM S63845 were used as a positive control for cleaved caspase-3 and cleaved PARP1.

corresponding reduction in GPX4 protein levels (Supplementary Fig. S12a, c). Inhibition of xCT was shown to reduce glutathione levels in GBM cells and thereby sensitise them to TMZ induced cytotoxicity [45]. Moreover, erastin was shown to sensitise glioma cells to TMZ induced cytotoxicity, and this was prevented by concurrent treatment with iron chelators [28]. Therefore, exploiting ferroptosis induced by small molecules and FDA-approved clinical drugs may be harnessed as an effective approach to treat apoptosis-resistant cancers [44]. To assess the impact of combining BH3 mimetic drugs with small molecule inducers of ferroptosis in GBM cells in culture, we first assessed the ability of RSL3 and erastin to induce ferroptosis as single agents, with cell viability determined by the MTT assay. In a dose dependent manner, erastin as well as RSL3 reduced the viability of U251 cells (IC_{50} with single agent treatment of erastin: 2.5 μM and RSL3; 64.5 nM), with significant rescue achieved by the addition of inhibitors of ferroptosis (1 μM liproxstatin-1 or 50 μM deferoxamine) (Fig. 7a, b). The combination treatment of the MCL-1 inhibitor S63845 and the BCL-XL inhibitor A1331852 with erastin (2, 2.5 and 3 μM) or RSL3 (50, 100 and 200 nM) for 24 h substantially diminished the viability of U251 cells, with a reduction in intracellular glutathione levels (Supplementary Fig. S10e, f), accumulation of cleaved (activated) caspase-3 and cleaved PARP1 (Supplementary Fig. S12b, d, e) with IC_{50} values markedly reduced compared to co-treatment with S63845 plus A1331852 (Fig. 7c-f). The status of mitochondria was examined in these experiments by assessing mitochondrial cytochrome *c* release and activation of BAX and BAK. After treatment with S63845 plus A1331852, both BAX and BAK were activated (Supplementary Fig. S13a) and cytochrome *c* was released from mitochondria (Supplementary Fig. S13b), indicative of mitochondrial outer membrane permeabilization (MOMP). This was not evident after treatment with erastin or RSL3, indicating that mitochondria remain intact during induction of ferroptosis. Interestingly, erastin and possibly RSL3 enhanced mitochondrial cytochrome *c* release when cells were also treated with S63845 plus A1331852; notably, this was not inhibited by liproxstatin-1 (Supplementary Fig. S13b). However, liproxstatin-1 (1 μM) could reduce the killing of U251 cells treated with increasing concentrations of S63845 plus A1331852 and fixed concentrations of erastin (2.5 μM) or RSL3 (100 nM) (Fig. 7e, f). We next explored the viability of U251 cells deficient in the effectors of apoptosis, BAX and BAK, after combination treatments with S63845 plus A1331852 on their own or when combined with erastin or RSL3. As expected, BAX/BAK DKO U251 cells were not killed by S63845 plus A1331852. They could, however, be killed when co-treated with these BH3 mimetic drugs plus erastin or RSL3, albeit to a much lesser extent compared to their parental counterparts (Fig. 7g, h). BAX/BAK DKO U251 cells co-treated with the ferroptosis inhibitor liproxstatin-1 were completely protected from killing induced by the combination of S63845 plus A1331852 with erastin or RSL3 (Fig. 7g, h). These findings demonstrate that inhibiting MCL-1 and BCL-XL with BH3 mimetic drugs cooperates with induction of ferroptosis by using erastin or RSL3 in killing U251 GBM cells.

DISCUSSION

The survival and quality of life of patients with GBM have not improved in the last 30 years. Lack of effective treatment options for these aggressive brain tumours largely falls on the micro-environmental and genetic features of the brain, frequently rendering these cancers inherently resistant to conventional and novel treatments [46]. In this study, we assessed the impact of combining BH3 mimetics with TMZ or other agents in a range of human GBM cell lines. Our findings show that co-targeting pro-survival proteins BCL-XL and MCL-1 with the BH3 mimetic drugs A1331852 and S63845, respectively, was more potent at triggering cell death in all six GBM cell lines tested, SNB-19, SNB-75, U251, SF268, SF295 and SF539, compared to conventional therapy with TMZ or the bromodomain inhibitor JQ1. This treatment with inhibitors of BCL-XL and MCL-1 was more robust at killing GBM cells compared to dual combination of inhibitors of MCL-1 and BCL-2 (Venetoclax/ABT-199), with significant cell death observed as early as 16 h with 0.1 μM of these BH3 mimetics. In U251 cells, significantly more killing was observed after treatment with combinations of a BCL-XL inhibitor with TMZ or JQ1 compared to exposure to TMZ or JQ1 as single agents, while combinations with an MCL-1 or a BCL-2 inhibitor did not enhance cell killing compared to single agent treatment.

U251 and SNB-19 cells both showed readily detectable cleavage (activation) of caspase-3 and cleavage of its substrate PARP1 in response to the various combination treatments. The p17 fragment of caspase-3 was more abundant in U251 cells, which is in accordance with this cell line being more sensitive to these treatments compared to SNB-19 cells. TMZ and JQ1 promote G2/M and G1 cell cycle arrest, respectively, in various cancer cell lines. Of note, we observed that in U251 cells, the BCL-XL inhibitor A1331852 diminished TMZ induced G2/M cell cycle arrest since large numbers of U251 cells exhibited a Sub-G1 DNA content after co-treatment with A1331852 plus TMZ, indicating that they were undergoing apoptosis. Overall, these data demonstrate that U251 and SNB-19 cells depend on BCL-XL and MCL-1 for survival and that combined inhibition of these pro-survival proteins with S63845 plus A1331852 or combined treatment with TMZ plus the BCL-XL inhibitor A1331852, cause significantly increased killing of GBM cells compared to standard of care therapy.

Previous studies have reported the impact of combining TMZ with the bromodomain inhibitor JQ1, with enhanced efficacy observed when these compounds were applied as a ligand-targeted liposomal nanocarrier in glioma cells in vitro and in intracranial orthotopic mouse models of GBM [35]. It was also shown that RNA-interference mediated reduction in BCL-2 or BCL-

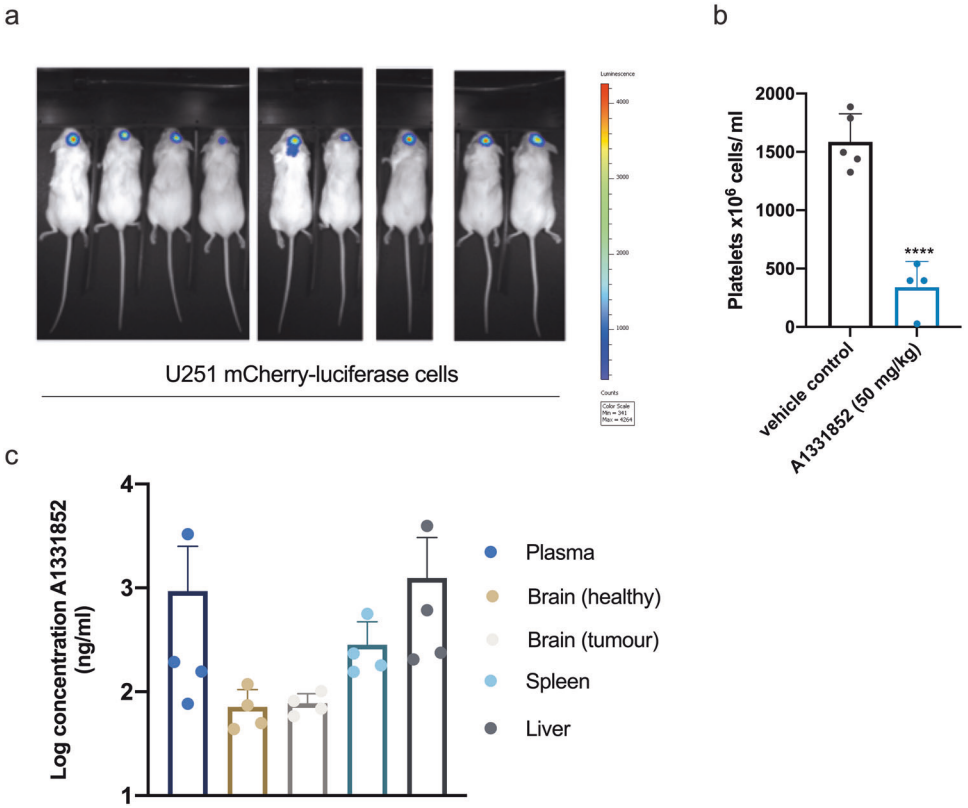

Fig. 6 A1331852 can penetrate the brain in an orthotopic mouse model of GBM. a NOD/SCID/$\gamma c^{-/-}$ mice were intra-cranially injected with 5×10^4 U251-mCh-Luc cells using a stereotactic frame. Successful engraftment and growth of tumour cells was detected on day 7 by bioluminescent imaging using the IVIS imaging system. **b** Platelet counts in wt NOD/SCID/$\gamma c^{-/-}$ mice intra-cranially injected with U251-mCh-Luc cells and then administered with vehicle (as a control) or 50 mg/kg body weight A1331852 (BCL-XL inhibitor) daily for 5 consecutive days. Blood was collected via cardiac puncture and shown are platelet counts 5 days post treatment. n = 5 wt NOD/SCID/$\gamma c^{-/-}$ mice administered with vehicle (as a control) and n = 4 wt NOD/SCID/$\gamma c^{-/-}$ mice administered with 50 mg/kg body weight A1331852 (BCL-XL inhibitor). Data are presented as mean ± s.d. student's unpaired t-test ****$P < 0.0001$. **c** Concentration of A1331852 in plasma, brain (healthy region or tumour region), spleen, and liver in tumour bearing mice following a 5-day treatment with this BH3 mimetic drug. Data are presented as mean ± s.d. n = 4 per tissue analysed.

XL was able to kill glioblastoma cells in culture, with cell killing shown to be caspase dependent [10]. Moreover, high levels of BCL-XL have been reported to be associated with rapid progression and poor survival of GBM patients. Therefore, BCL-XL has been proposed as a marker of therapy resistance in this malignancy [11]. In pre-clinical studies, the BCL-XL inhibitor A1331852 was shown to kill diverse lymphoma and leukaemia derived cell lines. Moreover, A1331852 could delay the progression of ALL in xenograft mouse models [20] and significantly inhibit tumour growth in xenograft models of certain solid cancers, including breast cancer, non-small cell lung cancer and ovarian cancer [47]. Combined targeting of BCL-XL and MCL-1 was reported to synergise in killing melanoma cells [21] and cervical cancer derived cell lines [22] in tissue culture. However, the clinical utility of dual BH3 mimetic treatment may be limited by their on-target toxicity in various healthy tissues that is predicted by experiments using genetic loss of these pro-survival proteins [48]. Notably, the loss of only single alleles of *Bcl-x* and *Mcl-1* causes fatal craniofacial defects [23], combined loss of BCL-XL and MCL-1 specifically in hepatocytes causes severe liver disease [24], and the on-target killing of platelets with ensuing thrombocytopenia limits the use of BCL-XL inhibitors in vivo [14, 15, 43]. Therefore, preclinical studies may need to focus on combinations of standard of care therapy with A1331852 or other BCL-XL inhibitors, such as those that have been modified (e.g., by conjugation to an antibody) or using PROTAC-based approaches [49] to selectively target malignant cells.

Under pathological conditions, such as GBM, the structural integrity of the BBB can be compromised, resulting in its disruption [50]. Despite these observations, clinical evidence demonstrates that there is a significant tumour burden with an intact BBB in GBM, compromising the entry of anti-cancer therapeutics [51], and this contributes to therapy resistance and tumour expansion. While BH3 mimetics are classified as 'small molecules', they are still relatively large, impeding their entry across the BBB. Nevertheless, we investigated if A1331852 can enter the brain in healthy mice and in an orthotopic mouse model of GBM. We report that A1331852 could penetrate the brain only in tumour bearing mice, entering both malignant as well as healthy tissues, albeit still at lower levels compared to other tissues. This reinforces the need for future studies to assess the in vivo impact of A1331852 and possibly other BH3 mimetic drugs in preclinical models of GBM.

Recent reports suggest that inducers of ferroptosis have anti-tumour effects in various experimental models of cancer [52–54], and they were shown to synergise with chemotherapeutic agents in killing diverse cancer cell lines [28, 55]. For example, it was reported that erastin sensitised GBM cells to TMZ by restraining xCT and cystathionine-γ-lyase function [28]. Many human cancer cell lines express high levels of xCT and this is often associated with enhanced tumour growth, metastasis, resistance to chemotherapy and poor patient survival [56, 57]. The tumour suppressor p53 was shown to inhibit cystine uptake and sensitise cells to ferroptosis by repressing expression of xCT in human

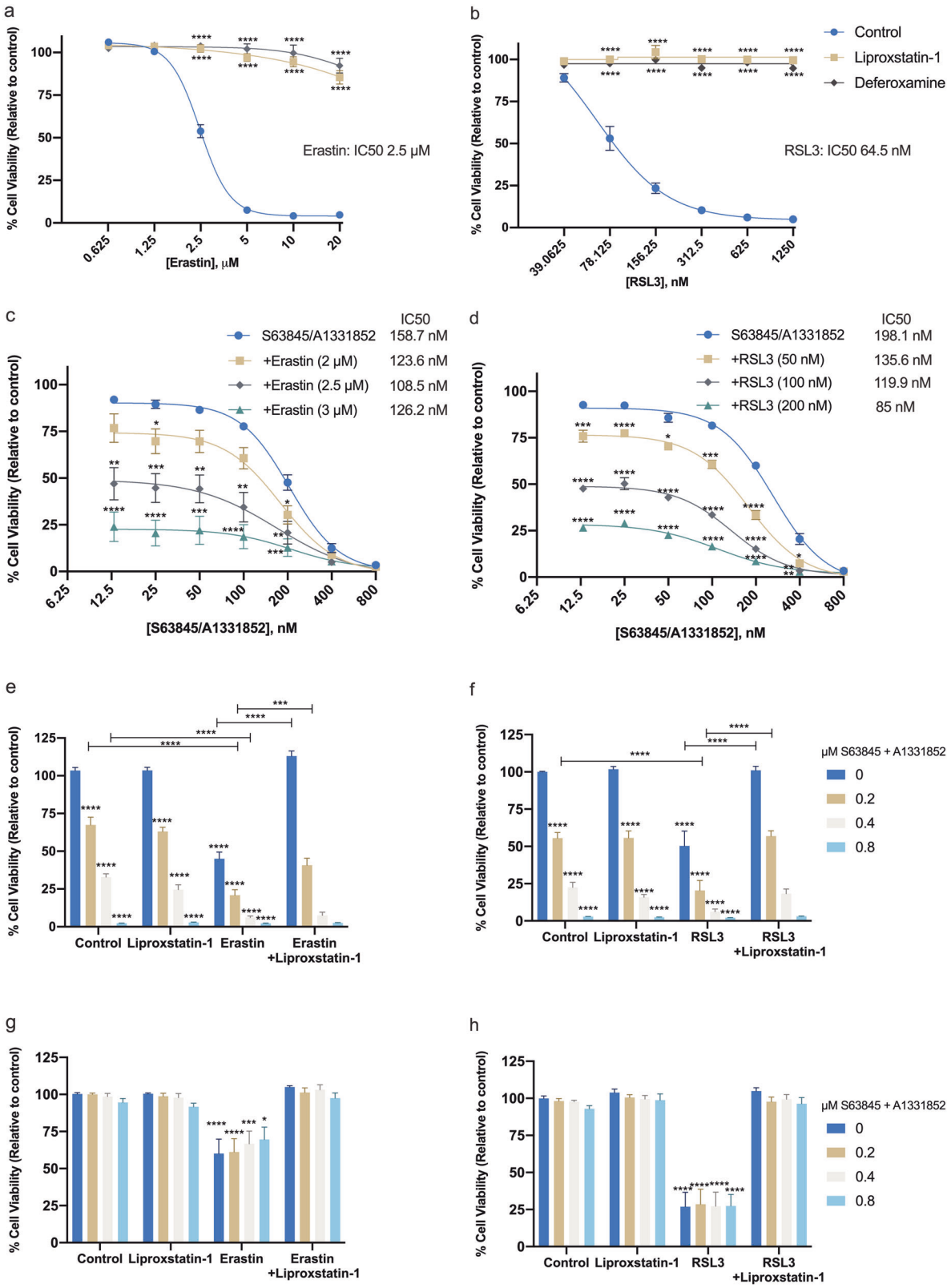

cancer cell lines [58]. Therefore, potent, and highly specific inhibitors of xCT are potentially interesting candidates for cancer therapy that are worth testing in preclinical studies.

Consistent with previous reports that glioblastoma cells are sensitive to inducers of ferroptosis, such as small molecule inhibitors of xCT or inhibitors of GPX4 [28, 59, 60], we found that erastin and RSL3 can kill U251 cells by inducing ferroptosis. Of note, our study is the first to report that BH3 mimetic drugs (S63845, A1331852) cooperate with inducers of ferroptosis (erastin or RSL3) in killing GBM cells, at least in vitro. While induction of ferroptosis by FDA-approved drugs, such as sulfasalazine and artesunate, holds promise for cancer therapy, a clinical trial of

Fig. 7 BH3 mimetic drugs cooperate with inducers of ferroptosis in the killing of GBM cells. a, **b** U251 cells were treated for 24 h with the indicated concentrations of erastin (**a**) or RSL3 (**b**) (both inducers of ferroptosis) ± 1 μM liproxstatin-1 or 50 μM deferoxamine (both inhibitors of ferroptosis). Cell viability was determined by using the MTT assay and data are expressed relative to vehicle control treated cells. Data are presented as means ± s.e.m; n = 9 from 3 independent experiments. One-way ANOVA with the Dunnet's multiple comparisons test. ****P < 0.0001. Data were fitted using a non-linear regression curve. **c**, **d** U251 cells were treated for 24 h with the indicated concentrations of S63845 (MCL-1 inhibitor) plus A1331852 (BCL-XL inhibitor) ± the indicated concentrations of erastin (**c**) or RSL3 (**d**). Cell survival was determined as described above. Data are presented as means ± s.e.m, n = 9 from 3 independent experiments. Two-way ANOVA with the Tukey's multiple comparisons tests relative to S63845 and A1331852 treated cells at the indicated concentrations; *P < 0.05, **P < ,0.01, ***P < 0.001, ****P < 0.0001. Data were fitted using a non-linear regression curve. **e**, **f** Parental U251 cells and **g**, **h** BAX/BAK DKO U251 cells were treated for 24 h with vehicle control, 0.2, 0.4 or 0.8 μM S63845 plus 0.2, 0.4 or 0.8 μM A1331852 ± 1 μM liproxstatin-1, ± 2.5 μM erastin (**e**, **g**) or 100 nM RSL3 (**f**, **h**). Cell survival was determined as described above. Data are presented as means ± s.e.m, n = 9 from 3 independent experiments. Two-way ANOVA with the Tukey's multiple comparisons tests relative to control or as indicated between treatment groups, *P < 0.05, **P < ,0.01, ***P < 0.001, ****P < 0.0001.

sulfasalazine for patients with glioma was unsuccessful due to severe side effects and lack of clinical response [61, 62]. Therefore, improved derivatives of erastin or other potent inducers of ferroptosis will need to be developed and tested in combination with inducers of apoptosis, such as BH3 mimetic drugs. Recently, imidazole ketone erastin was reported as a more metabolically stable inhibitor of system xCT and inducer of ferroptosis with nanomolar potency, and this compound was shown to delay tumour growth in a mouse xenograft model of diffuse large B cell lymphoma [63]. The safety and efficacy of imidazole ketone erastin in vivo was improved when nanocarriers were utilised, leading to more effective and selective delivery of this compound to tumour tissues [29]. However, the efficacy of imidazole ketone erastin in GBM cell lines (or other solid cancer derived cell lines) and in vivo models of GBM as single agent or in combination with standard of care chemotherapy is yet to be reported.

Recently, it was shown [64] that high expression of dihydroorotate dehydrogenase (DHODH), a key enzyme of de novo pyrimidine biosynthesis correlated with resistance to GPX4 inhibitors, such as RSL3 and ML162, in various cancer cell lines. Deletion of *DHODH* sensitised HT-1080 cells to RSL3 or ML162 induced lipid peroxidation and ferroptosis induced cell death. The therapeutic potential of brequinar, an inhibitor of DHODH was investigated using a HT-1080 cancer cell line xenograft mouse model. Knockdown of GPX4 sensitised HT-1080 tumours to brequinar treatment and suppressed tumour growth was largely restored by concomitant treatment with liproxstatin-1 [64]. While targeting DHODH in preclinical models of GBM is yet to be reported, the utility of DHODH inhibitor as an inducer of ferroptosis may be considered in combination with standard of care therapy for cancers. Indeed, future preclinical studies in orthotopic mouse models of GBM may involve evaluating the utility of combining an inducer of ferroptosis demonstrating in vivo efficacy in neurological disorders, a modified BCL-XL inhibitor that also demonstrates in vivo efficacy in neurological disorders and standard of care treatment in order to achieve neuroprotective outcomes and potent inhibition of brain cancer growth. Collectively, our findings demonstrate for the first time that combined treatment with BH3 mimetic drugs targeting MCL-1 and BCL-XL and small molecule inducers of ferroptosis, erastin or RSL3, elicited more potent killing of U251 cells compared to dual treatment with A1331852 plus S63845. This finding heralds dual triggering of apoptosis and ferroptosis as a novel treatment paradigm that may be harnessed for the development of improved therapies for GBM.

MATERIALS AND METHODS

Cell culture

SNB-19, SNB-75, U251, SF268, SF295 and SF539 cells were a kind gift from Associate Professors Andrew Morokoff and Kate Drummond (The University of Melbourne). U251 cells expressing mCherry and luciferase (U251-Ch-Luc) were generated by the transduction of U251 cells with a lentivirus encoding IRES mCherry Firefly luciferase, to enable in vivo tracking of tumour growth using bioluminescence. All cells were cultured in RPMI-1640 medium supplemented with 10% foetal bovine serum (FBS; MilliporeSigma), 100 U/mL penicillin, and 100 μg/mL streptomycin, and maintained at 5% CO_2, 37 °C. All cell lines were routinely verified as mycoplasma free.

CRISPR/Cas9 gene editing and cell sorting

CRISPR/Cas9 gene editing was performed by serial infection using a lentiviral system composed of stably expressed CAS9, followed by doxycycline-inducible expression of single guide RNA (sgRNA), as previously described [65]. A non-targeting control sgRNA (sgNT) or sgRNA construct against *Bax* and *Bak* were used [66]. To generate single-cell gene edited clones, cells with high expression of Cas9 (mCherry) and *Bax and Bak* or NT sgRNA (eGFP) were sorted into flat-bottomed 96-well plates at 1 cell per well on an Aria W flow cytometer (BD Biosciences). Twelve clones were expanded and sgRNA expression was induced with 1 μg/mL doxycycline for 5 days. Cells were screened for deletion of BAX and BAK by Western blot analysis.

Drug treatments

Cells were plated in triplicate at 1× 10^4 cells/well of flat-bottomed 24-well plates. Temozolomide (LKT LABS; #85622-93-1), JQ1 (Cayman Chemical #11187), Venetoclax/ABT-199 (BCL-2 inhibitor; Active Biochem; #A-1231), S63845 (MCL-1 inhibitor; Active Biochem; #6044), A-1331852 (BCL-XL inhibitor; AbbVie, provided by G. Lessene) in dimethyl sulfoxide (DMSO) and QVD-OPH (Enzo Life Sciences #502008362) were added at the specified concentrations. Cell viability was determined at the indicated time points. Data were normalised to control cells treated with an equivalent amount of DMSO (vehicle).

Cell cycle analysis

U251 and SNB-19 cells were treated with 50 μM TMZ, 1 μM JQ1 and 1 μM A1331852 or DMSO for 48 h and harvested by trypsinisation. Harvested cells were suspended in Hanks Balanced Salt Solution (HBSS) containing 2% FBS and fixed with 70% v/v ethanol for 24 h. Pelleted cells were washed twice with HBSS containing 2% FBS and then stained with 10 μg/mL DAPI in PBS for 30 min at room temperature in the dark. Stained cells were examined in a CytoFLEX (Beckman Coulter, Brea, USA) cytometer, and the data analysed using FlowJo software (BD Biosciences). The proportions of cells in the following cell cycle phases were determined: sub gap 1 (sub-G1; dead or dying); gap 1 (G_1); synthesis (S) and gap 2/mitosis (G_2/M).

Cell viability analysis

Cells were stained with Annexin V conjugated to alexa-647 or alexa-680 and DAPI and evaluated for apoptosis by flow cytometry according to the manufacturer's protocol (BD Biosciences Pharmingen, San Diego, CA, USA). Briefly, 1 × 10^5 cells were washed twice with PBS and stained with Annexin V alexa-647 or alexa-680 and DAPI (2 μg/mL) in 1× binding buffer (10 mM HEPES, pH 7.4, 140 mM NaOH, 2.5 mM $CaCl_2$) for 15 min at room temperature in the dark. The stained cells were examined in a CytoFLEX (Beckman Coulter, Brea, USA) flow cytometer and data were analysed using FlowJo software (BD Biosciences Pharmingen). Ten thousand events were analysed for each sample. GraphPad Prism software was used to calculate IC_{50} values.

MTT assay

Cell viability was measured using the 3-(4,5-dimethylthiazol-2-yl)-2,5-diphenyltetrazolium bromide (MTT) colorimetric assay as previously described [67]. Briefly, cells were cultured in 96-well plates at a density of 1×10^4 cells/well in growth medium for 16 h. Cells were subsequently incubated with ferroptosis inducing compounds (erastin, Selleckchem Cat#S7242; RSL3, Selleckchem Cat#S8155), apoptosis inducing compounds (S63845, A1331852) and/or ferroptosis preventing compounds (Liproxstatin-1, Sigma Aldrich Cat#SML1414; Deferoxamine, Sigma Aldrich Cat# D9533) at the indicated concentrations in growth medium for an additional 24 h. MTT was then added to the cultures at a final concentration of 0.5 mg/mL and absorbance was measured at 570 nm using a microplate reader (BioTek). Cell viability was expressed as a percentage of control cells. Non-linear regression analysis with a variable slope model was used to fit a four-parameter logistic curve to dose–response data to calculate EC_{50} with 95% CI (GraphPad Prism 9.0.0 software).

CellTitre-Glo assay

The CellTitre-Glo® assay was carried out according to the manufacturer's instructions. Briefly, CellTitre-Glo ATP reagent (Promega) was added to cells after treatment with the indicated agents to determine cell viability by measuring ATP levels. The luminescence of each sample was determined in a LumiSTAR Galaxy luminometer (BMG Labtech). Cell viability was expressed as percent change relative to DMSO (vehicle control) treated control cells.

Cell lysis, SDS PAGE and Western blot analysis

Untreated or drug-treated U251, and SNB-19 cells were harvested and lysed in radioimmunoprecipitation assay (RIPA) buffer (50 mM Tris-HCL, 150 mM NaCl, 1% NP-40, 0.5% DOC, 0.1% sodium dodecyl sulphate) supplemented with phosphatase inhibitors and complete protease inhibitor cocktail (Roche). Protein concentration was determined using the Pierce™ BCA Protein Assay Kit. Proteins were separated on 4-12% Bis-Tris NuPAGE protein gels (Invitrogen) under reducing conditions and then transferred onto Immobilon-P membranes. Membranes were blocked in PBS containing 0.1% Tween with 5% skim milk, then immunoblotted with antibodies to cleaved (activated) caspase-3 (Cell Signaling 9661), PARP1 (Abcam ab191217), MCL-1 (clone 19C4-15), BCL-XL (clone 9C9), BCL-2 (clone BCL-2-100), BAK (clone 4B5), BAX (clone 10F4) (all from the WEHI monoclonal antibody facility), GPX4 (Abcam ab125066), ACSL4 (sc-271800 Santa Cruz) and β-actin (loading control; Santa Cruz sc-517582 HRP) diluted in PBS containing 0.1% Tween. Secondary anti-rat/mouse/rabbit IgG antibodies conjugated to HRP (Southern BioTech) were applied, followed by Luminata Forte Western HRP substrate (Merck) for band visualisation. Membranes were imaged using the ChemiDoc XRS + machine with ImageLab software (Bio-Rad). Uncropped Western blots are provided in supplemental information.

Mice

6-week-old female non-obese diabetic/severe combined immunodeficient (NOD/SCID/$\gamma c^{-/-}$) mice were bred under specific pathogen-free conditions at the WEHI Kew animal facility and maintained in the animal facility at the Walter and Eliza Hall Institute of Medical Research (WEHI) (Parkville, Victoria, Australia). All mouse experiments were conducted with ethical approval from the WEHI animal ethics committee (ethics # 2020.022).

Administration of the BCL-XL inhibitor A1331852 in tumour naïve mice and in an orthotopic xenograft mouse model of GBM

For orthotopic xenograft mouse model of GBM, 5×10^4 U251-Ch-Luc cells were implanted intracranially using a stereotactic frame into 6-week-old female NOD/SCID/$\gamma c^{-/-}$ mice as previously described [42]. Engraftment of tumour cells was detected on day 7 by bioluminescent imaging using the IVIS imaging system (IVIS Lumina III Series Hardware, Perkin) as previously described [42]. After detectable engraftment of tumour cells, mice were gavaged with vehicle (control) or the BCL-XL inhibitor A1331852 (50 mg/kg body weight) formulated in 60% Phosal 50 PG (Lipoid), 27.5% polyethylene glycol 400 (Sigma), 10% ethanol, and 2.5% dimethyl sulfoxide (DMSO) daily for 5 consecutive days followed by blood and organ harvest. Mice not bearing tumours were gavaged once with the BCL-XL inhibitor A1331852 (25 mg/kg body weight), and organs as well as blood were collected 1 h and 4 h following drug administration. At experimental end point, mice were euthanised by CO_2 exposure, and brain, spleen and liver were collected and stored at −80 °C until UPLC analysis. Blood was drawn via cardiac puncture into microtainer tubes containing EDTA (Sarstedt, Ingle Farm, SA, Australia) and plasma was collected following centrifugation. Automated blood counts were carried out using an Advia 2120 haematological analyser (Siemens, Munich Germany).

Determination of plasma and organ concentrations of the BCL-XL inhibitor A1331852

Plasma and organ concentrations of A1331852 were determined via UPLC at the Monash Institute of Pharmaceutical Sciences. Briefly, a calibration standard curve was prepared from a stock solution of A1331852 (1 mg/mL in DMSO), with subsequent dilutions from the stock in 50% (v/v) acetonitrile in water. In-house plasma from male Swiss mice was used for preparation of the calibration standards and analytical replicates. Plasma calibration standards were prepared by spiking blank mouse plasma (50 µL) with the solution standards (10 µL) and the internal standard diazepam (10 µL of 5 µg/mL in 50% acetonitrile in water). Extraction from plasma samples was conducted using protein precipitation with acetonitrile (1:3 volume ratio). Standards and samples were vortexed and then centrifuged at 10,000 rpm for 3 min. The supernatant was subsequently separated and injected directly into the column for LC-MS/MS analysis. Brain and liver samples were quantified against calibration standards prepared using in-house brain and liver tissue from untreated male Swiss mice. Spleen samples were quantified using solvent calibration standards prepared in 50% acetonitrile in water. Pre-weighed tissue samples were homogenised using a gentle MACS™ homogeniser, in buffer containing stabilisation cocktail (0.1 M EDTA in 4 mg/mL potassium fluoride, 3 mL) cocktail/g tissue) before extraction with acetonitrile (1:3 volume ratio). Samples were vortexed and then centrifuged at 10,000 rpm for 3 min. The supernatant was subsequently separated and injected directly onto the column for LC-MS/MS analysis. Triplicate analytical replicate samples were prepared similarly to the standards for each sample type at three concentrations and repeat injections of these analytical replicate samples were included throughout the analytical run to assess assay performance. The extraction of the test compound from the standards and analytical replicate samples were conducted as described above.

Statistical analysis

Graphs were generated using GraphPad Prism software version 9.0.0 and was used for statistical analyses. Statistical analyses were performed using One-way ANOVA or Two-way ANOVA analysis of variance. Error bars represent the standard deviation (s.d.) of three independent experiments unless otherwise indicated (*$P < 0.05$, **$P < 0.01$, ***$P < 0.001$, ****$P < 0.0001$). For in vivo experiments, at least four mice were used per treatment group, no randomisation methods were applied for sample treatment allocations. For groups of mice analysed, no evidence for deviation of the data points from a normal distribution was found.

Ethics statement

All animal experiments complied with the regulatory standards of, and were approved by, The Walter and Eliza Hall Institute Animal Ethics Committee (Melbourne, Australia).

Supplementary information is available at the Cell Death and Differentiation website.

DATA AVAILABILITY

All data are available on request from the authors.

REFERENCES

1. Wolf KJ, Chen J, Coombes J, Aghi MK, Kumar S. Dissecting and rebuilding the glioblastoma microenvironment with engineered materials. Nat Rev Mater. 2019;4:651–68.
2. Sottoriva A, Spiteri I, Piccirillo SG, Touloumis A, Collins VP, Marioni JC, et al. Intratumor heterogeneity in human glioblastoma reflects cancer evolutionary dynamics. Proc Natl Acad Sci USA. 2013;110:4009–14.
3. Fisher JP, Adamson DC. Current FDA-approved therapies for high-grade malignant gliomas. Biomedicines. 2021;9:324–36.
4. Czabotar PE, Lessene G, Strasser A, Adams JM. Control of apoptosis by the BCL-2 protein family: implications for physiology and therapy. Nat Rev Mol Cell Biol. 2014;15:49–63.
5. Moujalled D, Strasser A, Liddell JR. Molecular mechanisms of cell death in neurological diseases. Cell Death Differ. 2021;28:2029–44.

6. Puthalakath H, Strasser A. Keeping killers on a tight leash: transcriptional and post-translational control of the pro-apoptotic activity of BH3-only proteins. Cell Death Differ. 2002;9:505–12.
7. Kelly GL, Strasser A. Toward targeting antiapoptotic MCL-1 for cancer therapy. Annu Rev Cancer Biol. 2020;4:299–313.
8. Singh R, Letai A, Sarosiek K. Regulation of apoptosis in health and disease: the balancing act of BCL-2 family proteins. Nat Rev Mol Cell Biol. 2019;20:175–93.
9. Cimini A, Ippoliti R. Innovative Therapies against human glioblastoma multiforme. ISRN Oncol. 2011;2011:787490.
10. Jiang Z, Zheng X, Rich KM. Down-regulation of Bcl-2 and Bcl-xL expression with bispecific antisense treatment in glioblastoma cell lines induce cell death. J Neurochem. 2003;84:273–81.
11. Liwak U, Jordan LE, Von-Holt SD, Singh P, Hanson JE, Lorimer IA, et al. Loss of PDCD4 contributes to enhanced chemoresistance in Glioblastoma multiforme through de-repression of Bcl-xL translation. Oncotarget. 2013;4:1365–72.
12. Milani M, Beckett AJ, Al-Zebeeby A, Luo X, Prior IA, Cohen GM, et al. DRP-1 functions independently of mitochondrial structural perturbations to facilitate BH3 mimetic-mediated apoptosis. Cell Death Discov. 2019;5:117.
13. Kotschy A, Szlavik Z, Murray J, Davidson J, Maragno AL, Le Toumelin-Braizat G, et al. The MCL1 inhibitor S63845 is tolerable and effective in diverse cancer models. Nature. 2016;538:477–82.
14. Lessene G, Czabotar PE, Sleebs BE, Zobel K, Lowes KN, Adams JM, et al. Structure-guided design of a selective BCL-X(L) inhibitor. Nat Chem Biol. 2013;9:390–7.
15. Souers AJ, Leverson JD, Boghaert ER, Ackler SL, Catron ND, Chen J, et al. ABT-199, a potent and selective BCL-2 inhibitor, achieves antitumor activity while sparing platelets. Nat Med. 2013;19:202–8.
16. Lin VS, Xu ZF, Huang DCS, Thijssen R. BH3 mimetics for the treatment of B-cell malignancies-insights and lessons from the clinic. Cancers. 2020;12:3353–76.
17. Caenepeel S, Brown SP, Belmontes B, Moody G, Keegan KS, Chui D, et al. AMG 176, a selective MCL1 inhibitor, is effective in hematologic cancer models alone and in combination with established therapies. Cancer Discov. 2018;8:1582–97.
18. Tron AE, Belmonte MA, Adam A, Aquila BM, Boise LH, Chiarparin E, et al. Discovery of Mcl-1-specific inhibitor AZD5991 and preclinical activity in multiple myeloma and acute myeloid leukemia. Nat Commun. 2018;9:5341.
19. Ramsey HE, Fischer MA, Lee T, Gorska AE, Arrate MP, Fuller L, et al. A novel MCL1 inhibitor combined with venetoclax rescues venetoclax-resistant acute myelogenous leukemia. Cancer Discov. 2018;8:1566–81.
20. Opferman JT. Attacking cancer's Achilles heel: antagonism of anti-apoptotic BCL-2 family members. FEBS J. 2016;283:2661–75.
21. Lee EF, Harris TJ, Tran S, Evangelista M, Arulananda S, John T, et al. BCL-XL and MCL-1 are the key BCL-2 family proteins in melanoma cell survival. Cell Death Dis. 2019;10:342.
22. Abdul Rahman SF, Muniandy K, Soo YK, Tiew EYH, Tan KX, Bates TE, et al. Co-inhibition of BCL-XL and MCL-1 with selective BCL-2 family inhibitors enhances cytotoxicity of cervical cancer cell lines. Biochem Biophys Rep. 2020;22:100756.
23. Grabow S, Delbridge AR, Aubrey BJ, Vandenberg CJ, Strasser A. Loss of a single Mcl-1 allele inhibits MYC-driven lymphomagenesis by sensitizing Pro-B cells to apoptosis. Cell Rep. 2016;14:2337–47.
24. Hikita H, Takehara T, Shimizu S, Kodama T, Li W, Miyagi T, et al. Mcl-1 and Bcl-xL cooperatively maintain integrity of hepatocytes in developing and adult murine liver. Hepatology. 2009;50:1217–26.
25. Merino D, Kelly GL, Lessene G, Wei AH, Roberts AW, Strasser A. BH3-mimetic drugs: blazing the trail for new cancer medicines. Cancer Cell. 2018;34:879–91.
26. Dixon SJ, Lemberg KM, Lamprecht MR, Skouta R, Zaitsev EM, Gleason CE, et al. Ferroptosis: an iron-dependent form of nonapoptotic cell death. Cell. 2012;149:1060–72.
27. Polewski MD, Reveron-Thornton RF, Cherryholmes GA, Marinov GK, Aboody KS. SLC7A11 overexpression in glioblastoma is associated with increased cancer stem cell-like properties. Stem Cells Dev. 2017;26:1236–46.
28. Chen L, Li X, Liu L, Yu B, Xue Y, Liu Y. Erastin sensitizes glioblastoma cells to temozolomide by restraining xCT and cystathionine-gamma-lyase function. Oncol Rep. 2015;33:1465–74.
29. Zhang Y, Tan H, Daniels JD, Zandkarimi F, Liu H, Brown LM. et al.Imidazole ketone erastin induces ferroptosis and slows tumor growth in a mouse lymphoma model.Cell Chem Biol. 2019;26:623–33. e9.
30. Stupp R, Mason WP, van den Bent MJ, Weller M, Fisher B, Taphoorn MJ, et al. Radiotherapy plus concomitant and adjuvant temozolomide for glioblastoma. N Engl J Med. 2005;352:987–96.
31. Floyd SR, Pacold ME, Huang Q, Clarke SM, Lam FC, Cannell IG, et al. The bromodomain protein Brd4 insulates chromatin from DNA damage signalling. Nature. 2013;498:246–50.
32. Li GQ, Guo WZ, Zhang Y, Seng JJ, Zhang HP, Ma XX, et al. Suppression of BRD4 inhibits human hepatocellular carcinoma by repressing MYC and enhancing BIM expression. Oncotarget. 2016;7:2462–74.
33. Ishida CT, Bianchetti E, Shu C, Halatsch ME, Westhoff MA, Karpel-Massler G, et al. BH3-mimetics and BET-inhibitors elicit enhanced lethality in malignant glioma. Oncotarget. 2017;8:29558–73.
34. Cheng Z, Gong Y, Ma Y, Lu K, Lu X, Pierce LA, et al. Inhibition of BET bromodomain targets genetically diverse glioblastoma. Clin Cancer Res. 2013;19:1748–59.
35. Lam FC, Morton SW, Wyckoff J, Vu Han TL, Hwang MK, Maffa A, et al. Enhanced efficacy of combined temozolomide and bromodomain inhibitor therapy for gliomas using targeted nanoparticles. Nat Commun. 2018;9:1991.
36. Tse C, Shoemaker AR, Adickes J, Anderson MG, Chen J, Jin S, et al. ABT-263: a potent and orally bioavailable Bcl-2 family inhibitor. Cancer Res. 2008;68:3421–8.
37. Zhang J, Stevens MF, Bradshaw TD. Temozolomide: mechanisms of action, repair and resistance. Curr Mol Pharm. 2012;5:102–14.
38. Shen W, Hu JA, Zheng JS. Mechanism of temozolomide-induced antitumour effects on glioma cells. J Int Med Res. 2014;42:164–72.
39. Delbridge AR, Strasser A. The BCL-2 protein family, BH3-mimetics and cancer therapy. Cell Death Differ. 2015;22:1071–80.
40. Strasser A, O'Connor L, Dixit VM. Apoptosis signaling. Annu Rev Biochem. 2000;69:217–45.
41. Yamaguchi H, Bhalla K, Wang HG. Bax plays a pivotal role in thapsigargin-induced apoptosis of human colon cancer HCT116 cells by controlling Smac/Diablo and Omi/HtrA2 release from mitochondria. Cancer Res. 2003;63:1483–9.
42. Abbott RC, Verdon DJ, Gracey FM, Hughes-Parry HE, Iliopoulos M, Watson KA, et al. Novel high-affinity EGFRvIII-specific chimeric antigen receptor T cells effectively eliminate human glioblastoma. Clin Transl Immunology 2021;10: e1283.
43. Mason KD, Carpinelli MR, Fletcher JI, Collinge JE, Hilton AA, Ellis S, et al. Programmed anuclear cell death delimits platelet life span. Cell. 2007;128:1173–86.
44. Hassannia B, Vandenabeele P, Vanden Berghe T. Targeting ferroptosis to iron out cancer. Cancer Cell. 2019;35:830–49.
45. Polewski MD, Reveron-Thornton RF, Cherryholmes GA, Marinov GK, Cassady K, Aboody KS. Increased expression of system xc- in glioblastoma confers an altered metabolic state and temozolomide resistance. Mol Cancer Res. 2016;14:1229–42.
46. Aldape K, Brindle KM, Chesler L, Chopra R, Gajjar A, Gilbert MR, et al. Challenges to curing primary brain tumours. Nat Rev Clin Oncol. 2019;16:509–20.
47. Leverson JD, Phillips DC, Mitten MJ, Boghaert ER, Diaz D, Tahir SK, et al. Exploiting selective BCL-2 family inhibitors to dissect cell survival dependencies and define improved strategies for cancer therapy. Sci Transl Med. 2015;7:279ra40.
48. Kehr S, Vogler M. It's time to die: BH3 mimetics in solid tumors. Biochim Biophys Acta Mol Cell Res. 2021;1868:118987.
49. Khan S, Zhang X, Lv D, Zhang Q, He Y, Zhang P, et al. A selective BCL-XL PROTAC degrader achieves safe and potent antitumor activity. Nat Med. 2019;25:1938–47.
50. van Tellingen O, Yetkin-Arik B, de Gooijer MC, Wesseling P, Wurdinger T, de Vries HE. Overcoming the blood-brain tumor barrier for effective glioblastoma treatment. Drug Resist Updat. 2015;19:1–12.
51. Sarkaria JN, Hu LS, Parney IF, Pafundi DH, Brinkmann DH, Laack NN, et al. Is the blood-brain barrier really disrupted in all glioblastomas? A critical assessment of existing clinical data. Neuro Oncol. 2018;20:184–91.
52. Yu Y, Xie Y, Cao L, Yang L, Yang M, Lotze MT, et al. The ferroptosis inducer erastin enhances sensitivity of acute myeloid leukemia cells to chemotherapeutic agents. Mol Cell Oncol. 2015;2:e1054549.
53. Gout PW, Buckley AR, Simms CR, Bruchovsky N. Sulfasalazine, a potent suppressor of lymphoma growth by inhibition of the x(c)- cystine transporter: a new action for an old drug. Leukemia. 2001;15:1633–40.
54. Liu DS, Duong CP, Haupt S, Montgomery KG, House CM, Azar WJ, et al. Inhibiting the system xC(-)/glutathione axis selectively targets cancers with mutant-p53 accumulation. Nat Commun. 2017;8:14844.
55. Sato M, Kusumi R, Hamashima S, Kobayashi S, Sasaki S, Komiyama Y, et al. The ferroptosis inducer erastin irreversibly inhibits system xc- and synergizes with cisplatin to increase cisplatin's cytotoxicity in cancer cells. Sci Rep. 2018;8:968.
56. Huang Y, Dai Z, Barbacioru C, Sadee W. Cystine-glutamate transporter SLC7A11 in cancer chemosensitivity and chemoresistance. Cancer Res. 2005;65:7446–54.
57. Koppula P, Zhuang L, Gan B. Cystine transporter SLC7A11/xCT in cancer: ferroptosis, nutrient dependency, and cancer therapy. Protein Cell. 2020;12:599–620.
58. Jiang L, Kon N, Li T, Wang SJ, Su T, Hibshoosh H, et al. Ferroptosis as a p53-mediated activity during tumour suppression. Nature. 2015;520:57–62.
59. Yang X, Liu J, Wang C, Cheng KK, Xu H, Li Q, et al. miR-18a promotes glioblastoma development by down-regulating ALOXE3-mediated ferroptotic and anti-migration activities. Oncogenesis. 2021;10:15.
60. Fan Z, Wirth AK, Chen D, Wruck CJ, Rauh M, Buchfelder M, et al. Nrf2-Keap1 pathway promotes cell proliferation and diminishes ferroptosis. Oncogenesis. 2017;6:e371.
61. Robe PA, Martin D, Albert A, Deprez M, Chariot A, Bours V. A phase 1-2, prospective, double blind, randomized study of the safety and efficacy of

Sulfasalazine for the treatment of progressing malignant gliomas: study protocol of [ISRCTN45828668]. BMC Cancer. 2006;6:29.
62. Robe PA, Martin DH, Nguyen-Khac MT, Artesi M, Deprez M, Albert A, et al. Early termination of ISRCTN45828668, a phase 1/2 prospective, randomized study of sulfasalazine for the treatment of progressing malignant gliomas in adults. BMC Cancer. 2009;9:372.
63. Larraufie MH, Yang WS, Jiang E, Thomas AG, Slusher BS, Stockwell BR. Incorporation of metabolically stable ketones into a small molecule probe to increase potency and water solubility. Bioorg Med Chem Lett. 2015;25:4787–92.
64. Mao C, Liu X, Zhang Y, Lei G, Yan Y, Lee H, et al. DHODH-mediated ferroptosis defence is a targetable vulnerability in cancer. Nature. 2021;593:586–90.
65. Aubrey BJ, Kelly GL, Kueh AJ, Brennan MS, O'Connor L, Milla L, et al. An inducible lentiviral guide RNA platform enables the identification of tumor-essential genes and tumor-promoting mutations in vivo. Cell Rep. 2015;10:1422–32.
66. Chin HS, Li MX, Tan IKL, Ninnis RL, Reljic B, Scicluna K, et al. VDAC2 enables BAX to mediate apoptosis and limit tumor development. Nat Commun. 2018;9:4976.
67. Southon A, Szostak K, Acevedo KM, Dent KA, Volitakis I, Belaidi AA, et al. Cu(II) (atsm) inhibits ferroptosis: Implications for treatment of neurodegenerative disease. Br J Pharm. 2020;177:656–67.

ACKNOWLEDGEMENTS

The authors thank Drs A Morokoff, K Drummond and M Rosenthal for human glioblastoma derived cell lines and discussions about our work.

AUTHOR CONTRIBUTIONS

DM designed, supervised, and performed research, analysed data, prepared figures, and wrote the manuscript. AS conceived, designed, supervised research, and wrote the manuscript. ES, AGS, FK, KB, MI, RSC, ZW, MS, RK and SG designed and performed some of the research that led to this work and analysed data. DN synthesised A1331852. MRJ, RK, GL and AIB contributed to discussions of the data. All authors reviewed the manuscript.

FUNDING

This work was supported by a Programme Grant (GNT1113133) to AS and GL, Research Fellowships (GNT1116937 to AS and GNT1117089 to GL) from the Australian NHMRC, the Leukemia & Lymphoma Society of America (Specialized Centre of Research [SCOR] grant no. 7015-18 to AS and GL), a grant-in-aid from the Cure Cancer Foundation (Australia), Leukaemia Foundation Australia grant (SG), the Lady Tata Memorial Trust (SG) and a grant from Cure Brain Cancer Australia grant (AS). Work in the laboratories of the authors was made possible through Victorian State Government Operational Infrastructure Support (OIS) and Australian Government NHMRC Independent Research Institute Infrastructure Support (IRIIS) Scheme.

COMPETING INTERESTS

DM, ES., KB, FK, MI, RSC, MRJ, DN, ZW, MXS, RMK, GL, SG and AS are or were employees of WEHI which receives royalties from AbbVie and Genentech from the sale of Venetoclax. GL and AS are collaborating with and have received funding from Servier for work on the development of MCL-1-specific BH3 mimetic drugs for cancer therapy. AIB is a shareholder in Alterity Ltd, Cogstate Ltd and Mesoblast Ltd. He is a paid consultant fee for, and has a profit share interest in Collaborative Medicinal Development Pty Ltd.

ADDITIONAL INFORMATION

Supplementary information The online version contains supplementary material available at https://doi.org/10.1038/s41418-022-00977-2.

Correspondence and requests for materials should be addressed to Diane Moujalled or Andreas Strasser.

Reprints and permission information is available at http://www.nature.com/reprints

Publisher's note Springer Nature remains neutral with regard to jurisdictional claims in published maps and institutional affiliations.